Received 24 May 2021; accepted 4 July 2021. Date of publication 12 July 2021; date of current version 21 July 2021.
The review of this article was arranged by Editor M. K. Radhakrishnan.

Digital Object Identifier 10.1109/JEDS.2021.3096389

Investigation on Stability of p-GaN HEMTs With an Indium–Tin–Oxide Gate Under Forward Gate Bias

CHIH-YAO CHANG [1] (Student Member, IEEE), YAO-LUEN SHEN [1] (Graduate Student Member, IEEE), CHING-YAO WANG [1] (Student Member, IEEE), SHUN-WEI TANG [2] (Student Member, IEEE), TIAN-LI WU [2] (Member, IEEE), WEI-HUNG KUO [3], SUH-FANG LIN [3], AND CHIH-FANG HUANG [1] (Senior Member, IEEE)

1 Institute of Electronics Engineering, National Tsing Hua University, Hsinchu 30013, Taiwan
2 International College of Semiconductor Technology, National Yang Ming Chiao Tung University, Hsinchu 30010, Taiwan
3 Electronics and Optoelectronics Research Laboratories, Industrial Technology Research Institute, Hsinchu 31040, Taiwan

CORRESPONDING AUTHORS: T.-L. WU AND C.-F. HUANG (e-mail: tlwu@nctu.edu.tw; cfhuang@ee.nthu.edu.tw)

This work was supported in part by the Ministry of Science and Technology (MOST), Taiwan, under Grant MOST 104-2221-E-007-079 and Grant 110-2622-8-009-018-SB, and in part by the Young Scholar Fellowship Program under Grant MOST 110-2636-E-009-023.

ABSTRACT In this study, p-GaN HEMTs with an indium-tin-oxide (ITO) electrode fabricated on the two different Mg concentration, i.e., 1×10^{19} cm^{-3} and 8×10^{19} cm^{-3},in p-GaN layer are investigated for the first time under the forward gate bias to understand the stability of the forward gate bias breakdown and V_{TH} shift stability. First of all, a Mg concentration in p-GaN layer results in a better Ohmic characteristic between the ITO and p-GaN contact. Furthermore, the fabricated device with a high Mg concentration of p-GaN layer shows a better forward gate breakdown voltage, which can be attributed to the better Ohmic characteristic between p-GaN and ITO electrode. Last, an obvious negative V_{TH} shift is observed, which is most probably related to the hole injections/trapping effects. In sum, the gate breakdown characteristic in p-GaN HEMTs with ITO electrode can be further improved while using high Mg concentration of p-GaN layer while an obvious a negative V_{TH} shift under a forward gate bias is observed, indicating a trade-off between the gate breakdown voltage and V_{TH} instability needs to be carefully considered to optimize the forward gate bias stability in p-GaN HEMTs with an ITO electrode.

INDEX TERMS GaN, high electron mobility transistor (HEMT), indium–tin–oxide gate electrode, PBTI.

I. INTRODUCTION

In recent years, p-GaN gate HEMTs show the promising performance and stability, which makes it one of the viable options for E-mode devices [1]–[3]. Regarding to the p-GaN gate, the gate contact on top of the p-GaN gate is one of the critical issues [4], [5]. In general, two different gate contacts on p-GaN gate are used, i.e., Schottky and Ohmic gate contact.

Compared to the Schottky contacts using TiN, Ni, or W electrode have been widely used and reported [5]–[8], the study on the Ohmic gate contacts are limited. So far, the Ohmic contact on top of the p-GaN is mainly formed by annealed Ni/Au, Pd, and other metallizations [9], [10]. In contrast with Schottky gate contact to a p-GaN gate HEMTs where a high electrical field appears in the metal/p-GaN junction depletion region under the forward gate bias, this high electric field will be absent in the ohmic gate contact approach, which is excepted to show improved gate reliability [11]–[13]. On the other hand, the ITO, which is well-known in using as the transparent conducting layer on p-GaN in LED fabrication [14], has been used to form an ohmic contact on top of the p-GaN [15], [16]. Therefore, ITO can be an alternative for the gate electrode in p-GaN gate HEMTs.

Recently, we have demonstrated the p-GaN/AlGaN/GaN HEMTs with an ITO gate electrode [17], showing a promising characteristic for power switching applications. However, the details of gate robustness, including the gate breakdown and positive bias temperature instability (PBTI) are still lacking for p-GaN HEMTs with an ITO gate electrode. Furthermore, the impacts of Mg concentration on the ITO/p-GaN contact and the device electrical characteristics are unknown. In this study, the p-GaN HEMTs with an ITO gate fabricated on two different epi structures, based on the conventional p-GaN/AlGaN/GaN HEMT structures. The major difference between these two epi structures is the surface Mg doping concentration of the p-GaN layer (Epi A: 1×10^{19} cm^{-3} and Epi B: 8×10^{19} cm^{-3}) that would affect the Ohmic contact characteristics of the ITO/p-GaN layer. Furthermore, the stability of p-GaN HEMTs with ITO gate electrode using two different Mg doping p-GaN layer is investigated under different forward gate bias.

II. DEVICE STRUCTURE AND EXPERIMENT DETAILS

Two epitaxies consisted of p-GaN/AlGaN/GaN HEMT structures were used in this study (named Epi A and Epi B). The epitaxies were grown on a 6-inch silicon substrate in a metal-organic chemical vapor deposition (MOCVD) system. From bottom to top, a $4.5 - \mu$m buffer and unintentionally doped GaN channel layer, a 12-nm $Al_{0.24}$ $Ga_{0.76}$ N barrier layer, and an 80-nm p-GaN layer. The Mg doping concentration of the p-GaN layer on Epi A is about 1×10^{19} cm^{-3}, while on Epi B is 8×10^{19} cm^{-3}.

After cleaning with a solvent, the definition of alignment marks was made via a chlorine-based dry etching process. After that, device isolation was formed via oxygen implantation. The depth of implantation around 300 nm which was based on SRIM simulation. Next, UV-ozone was used as a surface treatment for the p-GaN layer and then the sample was immersed in HCl : H_2 O (1:1) and BOE to clean the surface. A layer of 225-nm ITO was immediately deposited via the e-beam evaporator at a base pressure of 10^{-5} torr at 300^o C. Subsequently, a selective etch by chlorine-based ICP-RIE was performed until the AlGaN layer. Source and drain ohmic metal were formed by thermal evaporation of Ti/Al/Ti/Au (25/ 125/ 45/ 55 nm) followed by a rapid thermal annealing at 850°C for 30 seconds in a nitrogen ambient. The annealing process of contact of ITO/p-GaN, source electrode, and drain electrode completed simultaneously. Finally, a 30-nm Al_2 O_3 was used as the passivation layer.

The gate width (W_g) and the gate length (L_g) for the devices used in this study were 110 μm and 3 μm, respectively, with $L_{gs} = 5\mu$m and $L_{gd} = 15\mu$m. Fig. 1 is an illustration of the cross-section view for the p-GaN HEMTs with the ITO gate electrode.

III. RESULTS AND DISCUSION

The typical specific contact resistance of the ITO/p-GaN layer fabricated on Epi A and Epi B from TLM structure are $3.37 \times 10^0 \Omega$-cm^2 and $1.67 \times 10^{-1} \Omega$-cm^2, respectively, indicating that the device fabricated on Epi B has a low contact resistance, which is consistent with the p-GaN/AlGaN/GaN gate-to-source diode characteristics, as shown in Fig. 2. The current of diode fabricated on Epi B is much higher than Epi A (Fig. 2). These results indicate that a higher Mg doping concentration can lead to a low resistance between the ITO/p-GaN contact.

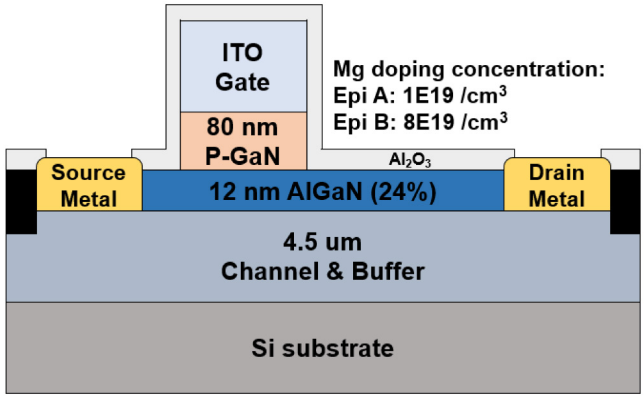

FIGURE 1. Schematic of the p-GaN/AlGaN/GaN HEMT with ITO gate electrode fabricated on two epi structures.

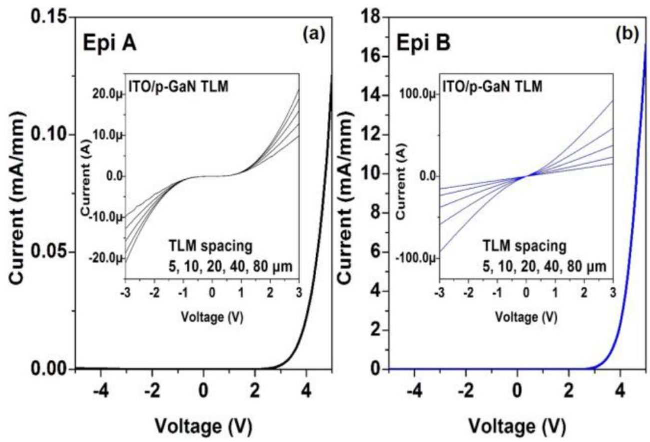

FIGURE 2. I-V comparison of the gate-to-source diodes of ITO p-GaN HEMT fabricated on (a) Epi A and (b) Epi B. The inset shows the TLM results of ITO/p-GaN contact on two cases.

The typical I_D-V_G and transconductance characteristics comparison were shown in Fig. 3. The maximum drain currents are 162 mA/mm and 248 mA/mm, while the threshold voltage extracted at I_D = 1mA/mm are 1.5 V and 1.2 V for the devices fabricated on Epi A and Epi B, respectively. A clear second g_m peak is observed for the device fabricated on Epi B, which is attributed to the hole injection, consistent with the reported literature for the p-GaN HEMTs with an ohmic contact [10]. In contrast, the g_m of device fabricated on Epi A is similar to the conventional p-GaN HEMTs by using the Schottky metals [8]. Fig. 4 shows the I_D-V_D curves of the ITO p-GaN gate HEMT fabricated on two epi structures. The maximum drain current and specific ON-resistance (R_{on}·A) for the two cases at V_G = 6 V are 210 mA/mm, 7.89 mΩ-cm^2 and 265 mA/mm, 6.4 mΩ-cm^2, respectively. The drain current of the device fabricated on Epi B is larger than Epi A, which may attribute to the higher level of hole

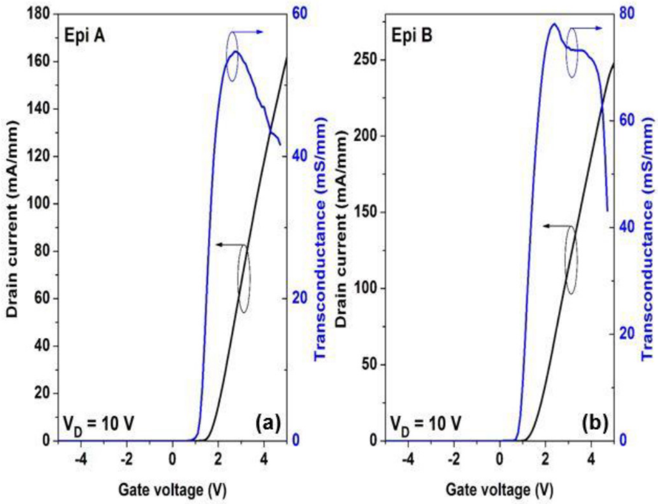

FIGURE 3. Comparison of I_D-V_G and transconductance of the fabricated ITO p-GaN HEMT on (a) Epi A and (b) Epi B.

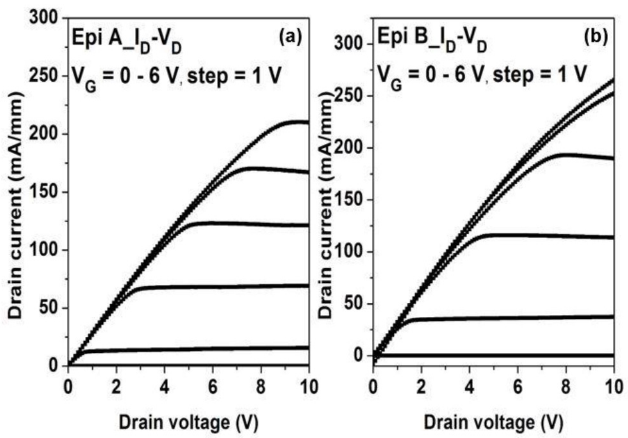

FIGURE 4. Comparison of I_D-V_D characteristics of the fabricated ITO p-GaN HEMT on (a) Epi A and (b) Epi B.

injection at the gate, induce conductivity modulation, and increasing the drain current [10].

The robustness of the ITO/p-GaN gate under the forward gate bias is evaluated by measure–sweep–measure sequence, where the procedure details are described in [17]. Fig. 5 shows the I_G-V_G monitored after each gate forward bias sweep and the summary of eight devices for each case. The result shows that the gate breakdown of the device fabricated on Epi B is much better than the device fabricated on Epi A, which indicated the Ohmic-like ITO/p-GaN contact has better gate robustness, consistent with the reported literature [11]–[13].

A measure-stress-measure technique was performed [18] to evaluate the V_{TH} instability of the devices under several gate biases as well. Fig. 6 shows the results in the fabricated devices on two epi structures. When the gate bias of $V_G = 3$ V, 4 V, and 5 V applied on the ITO p-GaN HEMT fabricated on Epi A, there is only less than 0.1 V of V_{TH} shift during the gate voltage stress, as shown in Fig. 6 (a).

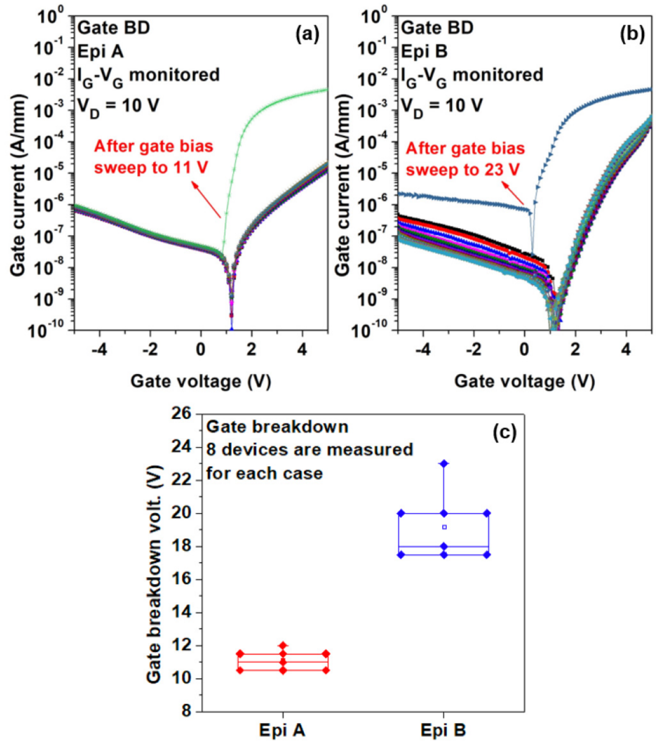

FIGURE 5. I_G-V_G curves monitored after each gate forward bias sweep of ITO p-GaN HEMT fabricated on (a) Epi A and (b) Epi B, and (c) shows the gate breakdown comparison results for two cases.

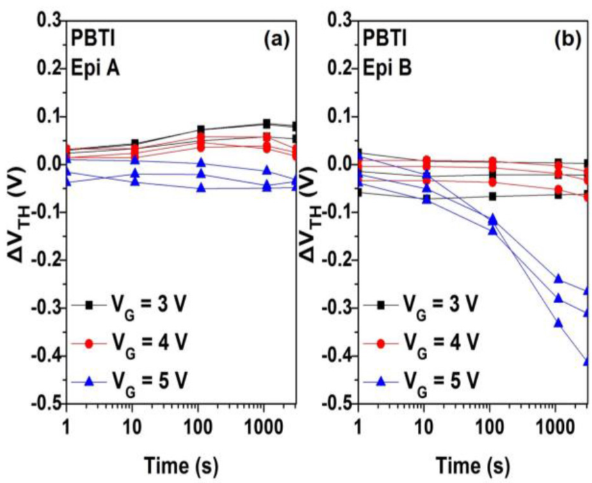

FIGURE 6. Delta V_{TH} versus stress time under several gate biases with the ITO p-GaN HEMT fabricated on (a) Epi A and (b) Epi B. Three devices were measured for each case and only used fresh devices.

However, in Fig. 6 (b), there is clear negative V_{TH} shift when gate bias $V_G = 5$ V applied on the devices fabricated on Epi B. Based on the aforementioned results, the p-GaN HEMT with in the Epi B, which has a higher Mg concentration, can have a hole injection phenomenon, which may induce the hole trapping at the p-GaN/AlGaN interface or at the AlGaN under the gate. Such hole trapping can lead to the increase of 2DEG density, further causing the negative V_{TH} shift during the gate stress.

IV. CONCLUSION

In this study, the forward gate bias breakdown and V_{TH} instability in p-GaN HEMTs with ITO gate electrodes on two different epi structures are investigated for the first time. First of all, the p-GaN HEMTs with a high Mg doping concentration shows a better Ohmic characteristic between ITO/p-GaN contact. The corresponding p-GaN HEMTs show a clear second peak of transconductance, which is related to the hole injection under the gate. Furthermore, the device with a better Ohmic characteristic between ITO/p-GaN shows a high breakdown voltage, which is most probably related to the absent of the electric field between gate metal/p-GaN. Furthermore, the V_{TH} stability is investigated in the device with two different Mg concentration. The results indicate that the device with a high Mg concentration shows an obvious negative V_{TH} shift, which is related to the hole injections/trapping effects. In sum, the gate stability in p-GaN HEMTs with ITO gate electrode is investigated, showing that a high Mg concentration in p-GaN layer can improve the gate breakdown characteristic but induce the obvious V_{TH} instability. Therefore, a trade-off between gate breakdown voltage and V_{TH} instability is needed to take into account to further optimize the p-GaN HEMTs with an ITO gate electrode.

REFERENCES

[1] D. Marcon, Y. N. Saripalli, and S. Decoutere, "200mm GaN-on-Si epitaxy and e-mode device technology," in *Proc. IEEE Int. Electron Devices Meeting*, Washington, DC, USA, Dec. 2015, pp. 16.2.1–16.2.4, doi: 10.1109/IEDM.2015.7409709.

[2] M. Meneghini *et al.*, "Reliability and failure analysis in power GaN-HEMTs: An overview," in *Proc. IEEE IRPS*, Monterey, CA, USA, Apr. 2017, pp. 3B2.1–3B2.8, doi: 10.1109/IRPS.2017.7936282.

[3] K. J. Chen *et al.*, "GaN-on-Si power technology: Device and applications," *IEEE Trans. Electron Devices*, vol. 64, no. 3, pp. 779–795, Mar. 2017, doi: 10.1109/TED.2017.2657579.

[4] F. Lee, L.-Y. Su, C.-H. Wang, Y.-R. Wu, and J. Huang, "Impact of gate metal on the performance of p-GaN/AlGaN/GaN high electron mobility transistors," *IEEE Electron Device Lett.*, vol. 36, no. 3, pp. 232–234, Mar. 2015, doi: 10.1109/LED.2015.2395454.

[5] I. Hwang *et al.*, "p-GaN gate HEMTs with tungsten gate metal for high threshold voltage and low gate current," *IEEE Electron Device Lett.*, vol. 34, no. 2, pp. 202–204, Feb. 2013, doi: 10.1109/LED.2012.2230312.

[6] N. E. Posthuma *et al.*, "An industry-ready 200 mm p-GaN E-mode GaN-on-Si power technology," in *Proc. IEEE 30th Int. Symp. Power Semicond. Devices ICs (ISPSD)*, Chicago, IL, USA, 2018, pp. 284–287, doi: 10.1109/ISPSD.2018.8393658.

[7] L. Sayadi, G. Iannaccone, S. Sicre, O. Häberlen, and G. Curatola, "Threshold voltage instability in p-GaN gate AlGaN/GaN HFETs," *IEEE Trans. Electron Devices*, vol. 65, no. 6, pp. 2454–2460, Jun. 2018, doi: 10.1109/TED.2018.2828702.

[8] T.-F. Chang *et al.*, "Phenomenon of drain current instability on p-GaN gate AlGaN/GaN HEMTs," *IEEE Trans. Electron Devices*, vol. 62, no. 2, pp. 339–345, Feb. 2015, doi: 10.1109/TED.2014.2352276.

[9] O. Hilt, F. Brunner, E. Cho, A. Knauer, E. Bahat-Treidel, and J. Würfl, "Normally-off high-voltage p-GaN gate GaN HFET with carbon-doped buffer," in *Proc. IEEE 23rd Int. Symp. Power Semicond. Devices ICs (ISPSD)*, San Diego, CA, USA, May. 2011, pp. 239–242, doi: 10.1109/ISPSD.2011.5890835.

[10] Y. Uemoto *et al.*, "Gate injection transistor (GIT)—A normally-off AlGaN/GaN power transistor using conductivity modulation," *IEEE Trans. Electron Devices*, vol. 54, no. 12, pp. 3393–3399, Dec. 2007, doi: 10.1109/TED.2007.908601.

[11] A. N. Tallarico *et al.*, "Investigation of the p-GaN gate breakdown in forward-biased GaN-based power HEMTs," *IEEE Electron Device Lett.*, vol. 38, no. 1, pp. 99–102, Jan. 2017, doi: 10.1109/LED.2016.2631640.

[12] I. Rossetto *et al.*, "Field- and current-driven degradation of GaN-based power HEMTs with p-GaN gate: Dependence on Mg-doping level," *Microelectron. Rel.*, vols. 76–77, pp. 298–303, Sep. 2017, doi: 10.1016/j.microrel.2017.06.061.

[13] M. Ruzzarin *et al.*, "Degradation mechanisms of GaN HEMTs with p-type gate under forward gate bias overstress," *IEEE Trans. Electron Devices*, vol. 65, no. 7, pp. 2778–2783, Jul. 2018, doi: 10.1109/TED.2018.2836460.

[14] Y. H. Lin, Y. S. Liu, and C. Y. Liu, "Light output enhancement of near UV-LED by using Ti-doped ITO transparent conducting layer," *IEEE Photon. Technol. Lett.*, vol. 22, no. 19, pp. 1443–1445, Oct. 2010, doi: 10.1109/LPT.2010.2056363.

[15] Y. C. Lin *et al.*, "InGaN/GaN light emitting diodes with Ni/Au, Ni/ITO and ITO p-type contacts," *Solid-State Electron.*, vol. 47, no. 5, pp. 849–853, May 2003, doi: 10.1016/S0038-1101(02)00440-9.

[16] D. W. Kim, Y. J. Sung, J. W. Park, and G. Y. Yeom, "A study of transparent indium tin oxide (ITO) contact to p-GaN," *Thin Solid Films*, vol. 398–399, pp. 87–92, Nov. 2001, doi: 10.1016/S0040-6090(01)01368-2.

[17] C.-Y. Chang *et al.*, "Demonstration of p-GaN/AlGaN/GaN high electron mobility transistors with an indium-tin-oxide gate electrode," *IEEE J. Electron Devices Soc.*, vol. 9, pp. 2–5, 2020, doi: 10.1109/JEDS.2020.3030911.

[18] T.-L. Wu *et al.*, "Toward understanding positive bias temperature instability in fully recessed-gate GaN MISFETs," *IEEE Trans. Electron Devices*, vol. 63, no. 5, pp. 1853–1860, May 2016, doi: 10.1109/TED.2016.2539341.